Influence of CeO_2 Thickness Layer Deposited on the 945A Steel Substrate Concerning the Corrosion Process

EDUARD SEBASTIAN BARCA[1], LUCIA CARMEN TRINCA[2], MIHAELA FILIPESCU[3], MARIA DINESCU[3], ADRIANA-GABRIELA PLAIASU[1], MARIOARA ABRUDEANU[1], RAZVAN LEATA*

[1] University of Pitesti, Faculty of Mechanics and Technology, Department of Manufacturing and Industrial Management,1 Tg din Vale Str, 110040, Arges, Romania

[2] Ion Ionescu de la Brad University of Agricultural Science and Veterinary Medicine, Faculty of Horticulture, Science Department, 3 Mihail Sadoveanu Alley, 700490, Ia°i, Romania

[3] National Institute for Lasers, Plasma and Radiation Physics, Lasers Department, 077125, Magurele, Romania

[4] University Dunarea de Jos, Faculty of Medicine, 47 Domneascã Str, 800008, Galaþi, Romania

The corrosion behaviour of four different preparations of pulsed laser deposition (PLD) CeO_2 coatings on 945A substrates in static 3.5% NaCl was investigated using linear polarization and electrochemical impedance spectroscopy (EIS). Four different nominal thicknesses were considered. The EIS proved this technique to be very suitable for the investigation of the electrochemical behavior, which is characterized by the dissolution characteristics of the coated materials. Because the coatings are porous, ionic paths between the electrolytic medium and the base substrate can eventually be produced, resulting in the corrosion of the coated material.

Keywords: 945A, CeO_2, pulsed laser deposition, EIS, SEM

In order to reduce fuel consumption and CO_2 emissions, the vehicle has to be lighter. Therefore thinner, lighter but still strong materials are used in the manufacture of the vehicles [1]. Having good mechanical properties of high strength and toughness, the high strength low alloy (HSLA) is being used in the automotive industry [2]. One of the problems encountered in automotive industry when using metallic parts for the frame of the vehicle is corrosion. CeO_2 was considered to be a suitable choice in depositing thin layers in order to provide corrosion protection by taking into consideration the physical and chemical properties it owns. Cerium belongs to the lanthanide series of chemical elements and it is the most spread rare earth element. Rare earth elements are considered to be rare because of the lack of concentrated ore bodies [3]. High thermal stability, high chemical stability, good adhesion, high melting point, high dielectric constant (26) , optical band gap with a value of 3.3 eV and high U.V. absorption have drawn attention on the possible applications CeO_2 might have [4-5]. Studies have been carried out for applications of the CeO_2, applications such as: corrosion resistance coatings, antireflection coatings, catalyst, electro chromic layers, fast oxygen sensors, antibacterial activity, microelectronics, optoelectronics and polishing material [6-11].

In the last two decades, a reliable and inexpensive method for obtaining thin films of simple or complex compounds was developed. This technique is Pulsed Laser Deposition – PLD, also called laser ablation [12]. The PLD method involves the interaction of the beam from a laser source with a target material (solid or liquid), producing plasma through which it is carried on a substrate, as a thin film [13].

This method has several advantages [12]: a) the deposition chamber is a "clean" reactor as the energy source (laser) is outside the reaction chamber, b) deposition process can be easily controlled because the processes involved are strongly influenced by laser parameters (wavelength, laser fluence, laser spot area, laser pulse duration, repetition rate, etc.), and this control is done from outside the reaction chamber, c) the thickness of the film can be controlled by the number of pulses that irradiate the material, d) laser radiation can be focused in very small spots which allows selective processing regions of interest, e) the transfer of the target to the substrate is stoechiometric, f) can produce new materials or in metastable states, that are impossible be achieved by other techniques.

Various techniques that were used to deposit nano CeO_2 are: sputtering, chemical vapour deposition, sol-gel deposition, spray pyrolysis and hydrothermal method [14-23].

The work aims to obtain corrosion protective layers through pulsed laser deposition on 945A steel used in the automotive industry especially on the frame of the vehicle which is subjected to corrosion.

Experimental part

Materials and samples preparation

Commercial CeO_2 micro sized ceria powder (99.9 % purity) was the starting point for the target preparation. The powder was compacted and sintered for 6 h in air at 1450 °C in order to obtain a dense ceramic target. The PLD process was carried out using an ArF laser, working at 193 nm wavelength with a frequency of 30 Hz. The target was irradiated in controlled oxygen gas flow at 0.1 mbar. In order to obtain crystalline thin films, the substrates were kept at 500 °C during the deposition process. The distance between target and substrate was set at 3.5 cm. The number of pulses was varied from 55.000 up to 220.000 for obtaining films with different thicknesses: 200 ± 35 (named Sample 1), 500 ± 55 (named Sample 2), 750 ± 70 nm (named Sample 3), and 1000 ± 90 nm (named Sample 4). Laser fluency was set at 3 J/cm^2 for all depositions. The depositions were carried out on 945A steel substrate that is used in the automotive industry.

In order to determine the deposition rate (the thickness of the ablated material deposited on the substrate during one laser pulse action), a thin film of CeO_2 was deposited

* *Tel.: (+40)0236427153*

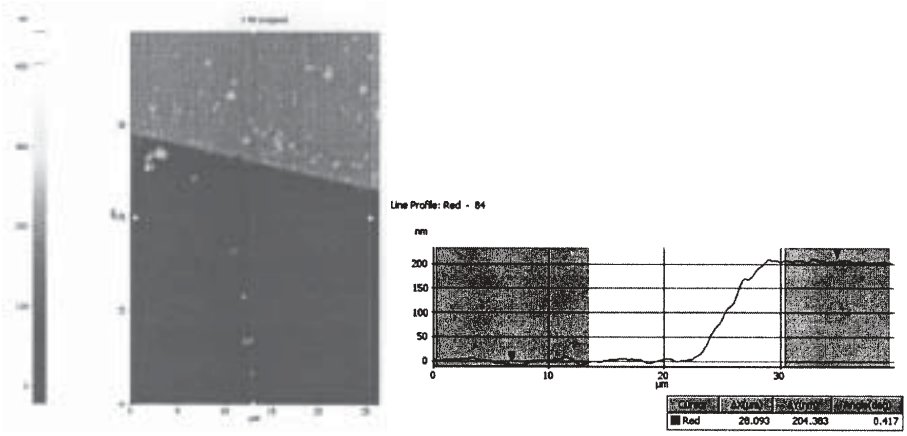

Fig. 1. AFM image and the profile for a sample of CeO_2 deposited on 945A steel substrate

on 945A steel substrate. Before the deposition, a partial area from the steel substrate was covered in order have a free ceria region. After the deposition, well defined areas with and without ceria film remained. The surface that contains area with film and without ceria film was scanned in order to determine the film thickness.

The height difference between the ceria thin film and steel substrate was around of 200 ± 35 nm (fig. 1). Therefore deposition rate (thickness divided at number of pulses) was calculated to be 0.05Å/pulse.

Electrochemical method

Corrosion tests were performed electrochemically at room temperature (25 ± 1°C) in a 3.5% NaCl in distilled water.

The tests specimens was placed in a glass corrosion cell, which was filled with freshly prepared electrolyte. A saturated calomel electrode (SCE) was used as the reference electrode and a platinum coil as the counter electrode. All potentials referred to in this article are with respect to SCE. The measurement was managed by a PAR 4000 potentiostat controlled by a personal computer with dedicate software (PowerCorr).

EIS measurements were performed after the samples were immersed in electrolyte at open circuit potential, for different period of times: 1 hour, 1 day, and 7 days. The alternating current (AC) impedance spectra for samples were obtained with a scan frequency range of 100 kHz to 10 mHz with amplitude of 10 mV. In order to supply quantitative support for discussions of these experimental EIS results, an appropriate model (ZSimpWin-PAR, USA) for equivalent circuit (EC) quantification has also been used. The usual guidelines for the selection of the best-fit EC were followed: a minimum number of circuit elements are employed and the χ^2 error was suitably low ($\chi^2 < 10^{-4}$), and the error associated with each element was up to 5%. Instead of pure capacitors, constant phase elements (CPE) were introduced in the fitting procedure to obtain good agreement between the simulated and experimental data [24-27].

Measurement of linear potentiodynamic polarization curves was initiated after 7 days exposure to the test environment. These tests were conducted by stepping the potential using a scanning rate of 1 mV/s from -1500 mV (SCE) to 0 mV (SCE). The potentiodynamic polarization curves were plotted, and the corresponding values for the zero current potential (ZCP), and the corrosion current density (i_{corr}), were determined from them.

Results and discussions

The Nyquist impedance diagrams for 945A coated samples in 3.5% NaCl solution as a function of immersion time are shown in figure 2 A-D.

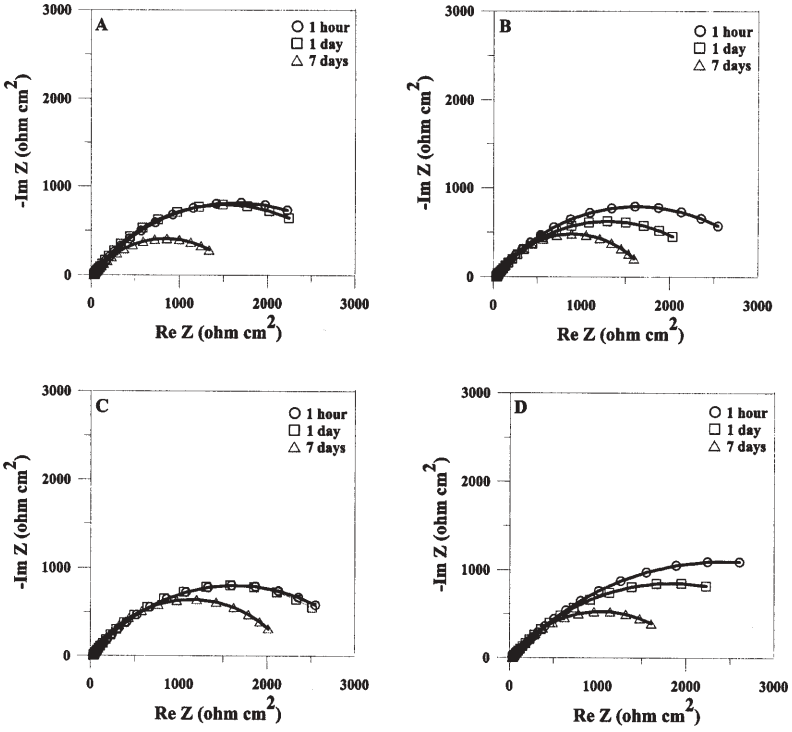

Fig. 2. Electrochemical impedance diagrams for: (A) sample 1, (B) sample 2, (C) sample 3, and (D) sample 4 as a function of immersion time in 3.5% NaCl solution at open circuit potential

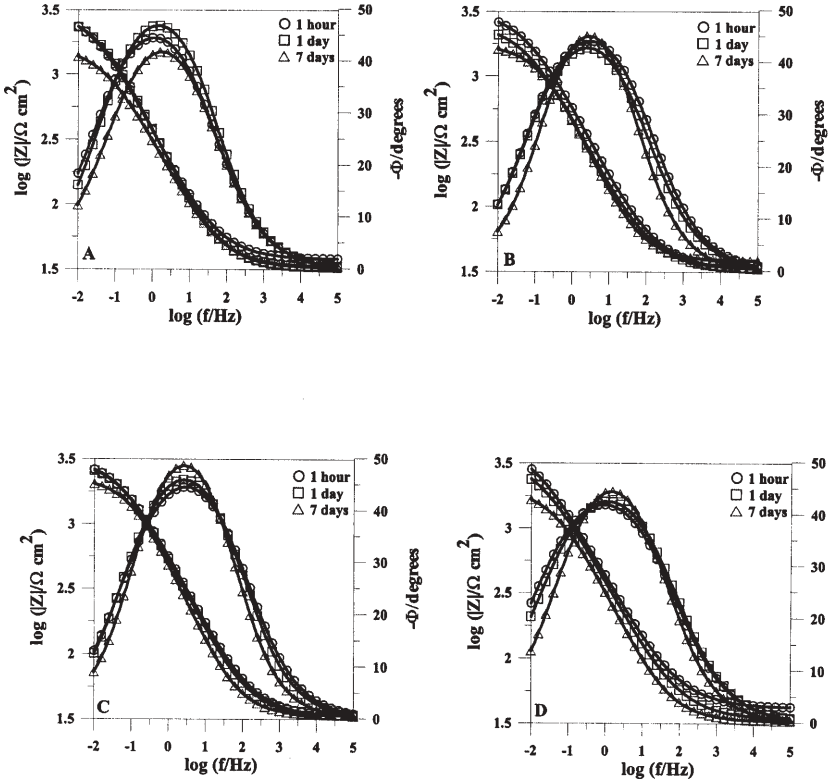

Fig. 3. Bode plots for EIS data: (A) sample 1, (B) sample 2, (C) sample 3, and (D) sample 4 as a function of immersion time in 3.5% NaCl solution at open circuit potential

All the diagrams for coated samples show a capacitive arc. The capacitive arc could be relating the electric double layer capacitance at the electrode/solution interface, which includes the formed film-solution interface. The diameters of the semicircles correspond to the polarizing resistance (R_p) indicative of the kinetics of the charge transfer reactions or rate of dissolution. It could be observed from the figures 2 A-D that after 7 days of immersion in 3.5% NaCl solution, the diameter of the semicircle of all samples decreased. The decrease in diameter indicates a decrease in corrosion resistance. figure 3 A-D shows the Bode diagrams for the same systems.

Within the intermediate frequency range, the Bode diagrams show straight lines with slopes smaller than the value -1 and a phase angle smaller than 90°. These features as well as flat capacitive arcs are relating with the frequency dispersion and can be attributing to inhomogeneities of the solid surface.

According to the impedance diagram, the Bode-phase plots are in agreement with an EC with one time constant (fig. 4).

Fig. 4 . Equivalent circuit (EC) used for fitting the measured impedance spectra

The impedance spectra were fitted using the ZSimpWin software and the resultant EIS parameters are given in Table 1. The fitting quality of EIS data was estimated by both the chi-square (χ^2) test (between 10^{-4} and 10^{-5}) values and the comparison between error distribution versus frequency values (±5% for the whole frequency range) corresponding to experimental and simulated data. In this EC, R_{sol} is the ohmic resistance of the electrolyte (around 40 Ω cm^2), R_p represents the polarization resistance and Q is the impedance related to a constant phase element (CPE).

The more the value of polarization resistance increases, the more the sample will resist corrosion.

From Stern-Geary equation [28],

$$i_{corr} = \frac{B}{R_p}$$

with B constant determined by Tafel slope tests, it follows that the higher the R_p, the lower is the corrosion rate.

For all coated samples, the EIS spectra indicate that the formed film is affected by the solution with the increase of immersion time, as suggested by the decrease of polarization resistance (R_p) values. The R_p values are higher on CeO_2 coated thicker layer sample is more corrosion resistant than on CeO_2 coated thinner layer sample.

The Q values increase by increasing the immersion time assuming values characteristics of the electric double layer. These results indicate that the solution reaches for all coated samples surface because of the formed film dissolution causing the decrease of the total systems impedance. This hypothesis could be confirmed by the decreasing time of the capacitive arcs in the Nyquist diagrams (fig. 2).

Table 1

ELECTROCHEMICAL PARAMETERS OBTAINED FROM EIS SPECTRA USING THE SELECTED EC FOR THE CeO_2 COATED SAMPLES AFTER DIFFERENT IMMERSION TIME IN 3.5% NACL SOLUTION AT OPEN CIRCUIT POTENTIAL

potential				
Samples	Immersion time	10^4Q, S cm^{-2} s^n	n	$10^{-3}R_p$, Ω cm^2
Sample 1	1 hour	1.2	0.80	2.4
	1 day	1.3	0.79	2.1
	7 days	1.7	0.77	1.4
Sample 2	1 hour	1.1	0.80	2.6
	1 day	1.2	0.78	2.3
	7 days	1.7	0.77	1.5
Sample 3	1 hour	1.1	0.80	2.9
	1 day	1.3	0.79	2.4
	7 days	1.6	0.78	1.7
Sample 4	1 hour	1.1	0.81	3.1
	1 day	1.2	0.80	2.6
	7 days	1.5	0.79	1.8

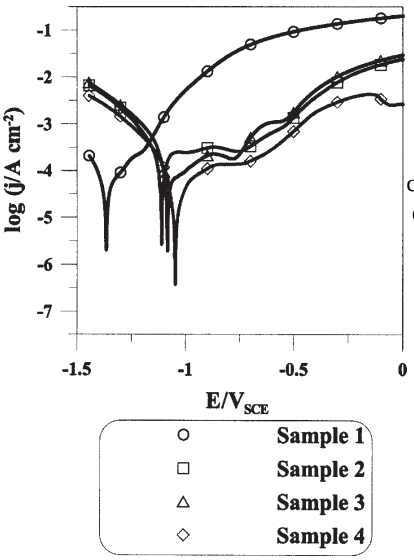

Fig. 5. Linear potentiodynamic polarization curves measured for CeO_2 coated specimens after 7 days immersion in 3.5% NaCl

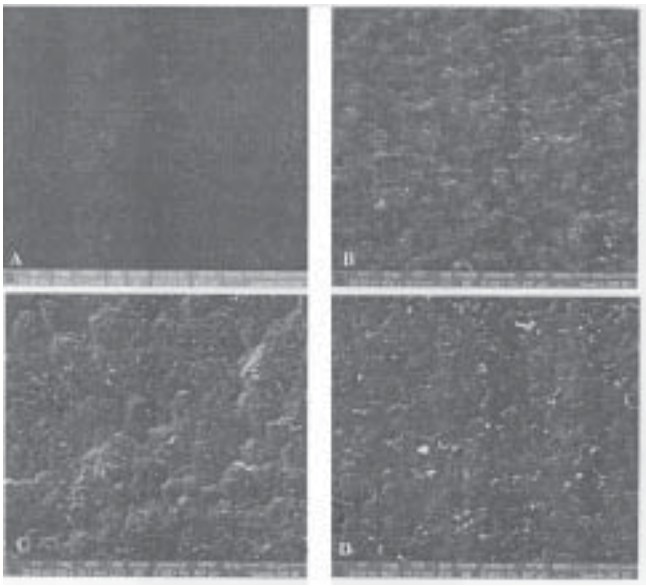

Fig. 6. SEM observation of the: (A) sample 1, (B) sample 2, (C) sample 3, and (D) sample 4 after linear polarization test in 3.5% NaCl solution

Figure 5 displays the linear polarization curves, in semi-logarithmic scale of current densities corresponding to coating samples in 3.5% NaCl solution at 25 °C traced between – 1500 mV to 0 mV with 1 mV/s potential sweep rate. Figure 5 indicates that the CeO_2 coatings sample presents a similar anodic behaviour. No passive region was observed, the anodic current density continuously increased. Such effect has been associated to the diffusion of small Cl^- ions than that of the oxygen, which makes difficult for the surface to be homogeneously passivated. The average values zero corrosion potential (ZCP) and corrosion current density (i_{corr}) from polarization curves determined by the PowerCorr software are presented in table 2.

The linear polarization curves of sample 4 showed a shift of ZCP to more positive value (-1045 mV) compared with sample 1 (-1365 mV). The higher ZCP exhibited, probably can be associated with the positive contribution of the thickness of the deposited layer. The corrosion current density for sample 1 is ca. two times higher than for sample 4. Thus, the results indicated that the sample 1 is most easily corroded.

Figure 6 displays the SEM images of coated surface samples after linear potentiodynamic polarization test at 0 mV in 3.5% NaCl solution. The common susceptible sites

Table 2

THE MEAN VALUES OF PARAMETERS MEASURED AND CALCULATED FOR THE SAMPLES IN 3.5% NaCl SOLUTION (25 °C)

Specimens	ZCP (mV)	i_{corr} (μA/cm^2)
Sample 1	-1365	107
Sample 2	-1109	83
Sample 3	-1082	71
Sample 4	-1045	45

for pits are known to be the inclusions, second phase precipitates, processing defects such as pores, cracks, etc.

Conclusions

The aim of this paper is the improving of materials properties by coating. In our researches we have accomplished some experiments to establish some properties of the materials obtained. The electrochemical behavior of PLD Ceo_2 coatings on 945A steel substrate was evaluated by means of linear polarization and EIS in 3.5% NaCl solution, at 25 °C. The zero corrosion potential (ZCP) of an sample 4 is nobler than of sample 1, and the corrosion current density (i_{corr}) of sample 1 is more than two times larger than that of sample 4. For all coated samples, the polarization resistance (R_p) values obtained from EIS spectra, decreases slowly with the time of electrode immersion.

Acknowledgement: This work of Bârcã Eduard Sebastian was supported by the strategic grant POSDRU/159/1.5/S/138963 - PERFORM, co-financed by the European Social Fund – Investing in People, within the Sectoral Operational Programme Human Resources Development 2007-2013.

References

1. PARKES D., XU W., WESTERBAAN D., NAYAK S.S., ZHOU Y., GOODWIN F., BHOLE S., CHEN D.L. - Microstructure and fatigue properties of fiber laser welded dissimilar joints between high strength low alloy and dual-phase steels - Mat. and Des. 51, 2013, p. 665
2. KANG J., WANG C., WANG G.D. - Microstructural characteristics and impact fracture behavior of a high-strength low-alloy steel treated by intercritical heat treatment - Mat. Sci. and Eng. A 553, 2012, p. 96
3. CASTANO E. C., O'KEEFE J. M., FAHRENHOLTZ W. G. - Cerium-based oxide coatings - Curr. Op.in Sol. St. and Mat. Sci. 19, 2015, p 69
4. GUHEL Y., TOLOSHNIAK T., BERNARD J., BESQ A., COQ GERMANICUS R., ELFALLAH J., PESANT J.C., DESCAMPS P., BOUDART B. - Rapid thermal annealing of cerium dioxide thin films sputtered onto silicon(111) substrates: Influence of heating rate on microstructure and electrical properties - Mat. Sci. in Semi. Pro. 30, 2015, p. 352;
5. BALAKRISHNAN G., TRIPURA SUNDARI S., KUPPUSAMI P., CHANDRA MOHAN P., SRINIVASAN M.P., MOHANDAS E., GANESAN V., SASTIKUMAR D. - A study of microstructural and optical properties of nanocrystalline ceria thin films prepared by pulsed laser deposition - Thin Sol. Fil. 519, 2011, p. 2520;
6. PARK I.-W., LIN J., MOORE J. J., KHAFIZOV M., HURLEY D., MANUEL M. V., ALLEN T. - Grain growth and mechanical properties of CeO2-x films deposited on Si(100) substrates by pulsed dc magnetron sputtering - Surf. & Coat. Tech. 217, 2013, p. 34;
7. PATIL B.B., PAWAR S.H. - Structural, morphological and electrical properties of spray deposited nano-crystalline CeO2 thin films - J. of All. and Comp. 509, 2011, p. 414;
8. SUN C., LI H., WANG Z.X., CHEN L., HUANG X. - Synthesis and Characterization of Polycrystalline CeO2 Nanowires - Chem. Lett. Vol.33, No.6, 2004, p. 662 ;
9. ANWAR M.S., KUMAR S., AHMED F., ARSHI N., KIL G.S., PARK D.W., CHANG J., KOO B. H. - Hydrothermal synthesis and indication of

room temperature ferromagnetism in CeO2 nanowires - Mat. Lett. 65, 2011, p. 3098;
10. XU C. and QU X. - Cerium oxide nanoparticle: a remarkably versatile rare earth nanomaterial for biological applications - NPG Asia Materials 6, 2014, p. 1;
11. NAGANUMA T., TRAVERSA E. - The effect of cerium valence states at cerium oxide nanoparticle surfaces on cell proliferation - Bio. 35, 2014, p. 4441;
12. CHRISEY D.B., HUBLER G.K., Pulsed Laser Deposition of Thin Films, New York, 1944. p. 115;
13. BRODOCEANU D., SCARISOREANU N.D., (MORAR) FILIPESCU M., EPURESCU G.N., MATEI D.G., VERARDI P., CRACIUN F., DINESCU M. - Pulsed laser deposition of oxide thinfilms, in: Plasma Production by Laser Ablation, PPLA 2003, W. Sci, 2004, p. 41;
14.KUMAR K.-N. P., TRANTO J., NAIR B. N., KUMAR J., HØJ J. W., ENGELL J. E. - Effect of sintering atmosphere on the pore-structure stability of cerium doped nanostructured alumina, Mater. Res. Bull. 29, 1994, p. 551;
15. POLYCHRONOPOULOU K., FIERRO J. L. G., EFSTATHIOU A. M. - The phenol steam reforming reaction over MgO-based supported Rh catalysts, J. Catal. 28, 2004, p. 417;
16. POLYCHRONOPOULOU K., COSTA C. N., EFSTATHIOU A. M. - The steam reforming of phenol reaction over supported-Rh catalysts Appl. Catal. A 37, 2004, p. 272 ;
17. CORMA A., ATIENZAR P., GARC´IA H., CHANE-CHING J.-Y. - Hierarchically mesostructured doped CeO2 with potential for solar-cell use, Nat. Mater. 3, 2004, p. 394;
18. MASUI T., YAMAMOTO M., SAKATA T., MORI H., ADACHI G. - Synthesis of BN-coated CeO2 fine powder as a new UV blocking material J. Mater. Chem. 10, 2000, p. 353;
19. BOUCHAUD B., BALMAIN J., BONNET G., PEDRAZA F. - Optimizing structural and compositional properties of electrodeposited ceria coatings for enhanced oxidation resistance of a nickel-based superalloy - App. Surf. Sci. 268, 2013, p. 218;
20. KANG H.S., KANG Y.C., KOO H.Y., JU S.H., KIM D.Y., HONG S.K., et al. - Nano-sized ceria particles prepared by spray pyrolysis using polymeric precursor solution, Mater. Sci. Eng. B 127, 2006, p. 99 ;
21. MULLINS D.R., OVERBURY S.H., HUNTLEY D.R., Electron spectroscopy of single crystal and polycrystalline cerium oxide surfaces, Surf. Sci. 409, 1998, p. 307;
22. WANG H.P., ZHANG H. L., ZHANG H., BAI J.F., REN J.S., WANG S.J. - CeO2 films epitaxially grown on SrTiO3 substrates by pulsed laser deposition using a metallic Ce target ; Vac., 2013, p. 87;
23. CHO Y.J., JANG H., LEE K.-S., KIM D.R. - Direct growth of cerium oxide nanorods on diverse substrates for superhydrophobicity and corrosion resistance, App. Surf. Sci. 340, 2015, p. 96;
24. BOLAT G., IZQUIERDO J., GLORIANT T., CHELARIU R., MARECI D., SOUTO R.M., Corr. Sci. 98, 2015, p. 170;
25. MINCIUNA M.G., VIZUREANU P., ACHITEI D.C., GHIBAN B., SANDU A.V., MARECI D., BALAN A., Rev Chim. (Bucharest), **65**, no. 10, 2014, p. 1138;
26. MARECI D., CHELARIU R., IVANESCU S., GORDIN D.M., CRETESCU I., GLORIANT T., Rev Chim. (Bucharest), **60** no. 8, 2009, p. 787;
27. MARECI D., EARAR K., ZETU I., BOLAT G., CRIMU C., ISTRATE B., MUNTEANU C., MATEI M.N., Mat. Plast., **52**, no. 2, 2015, p. 150;
28. STERN M., GEARY A., J. Electrochem. Soc., 104, 1957, p. 56.

Manuscript received: 18.09.2015